Absence of anomalous Nernst effect in spin Seebeck effect of Pt/YIG

B. F. Miao, S. Y. Huang, D. Qu, et al.

View Online   Export Citation   CrossMark

ARTICLES YOU MAY BE INTERESTED IN
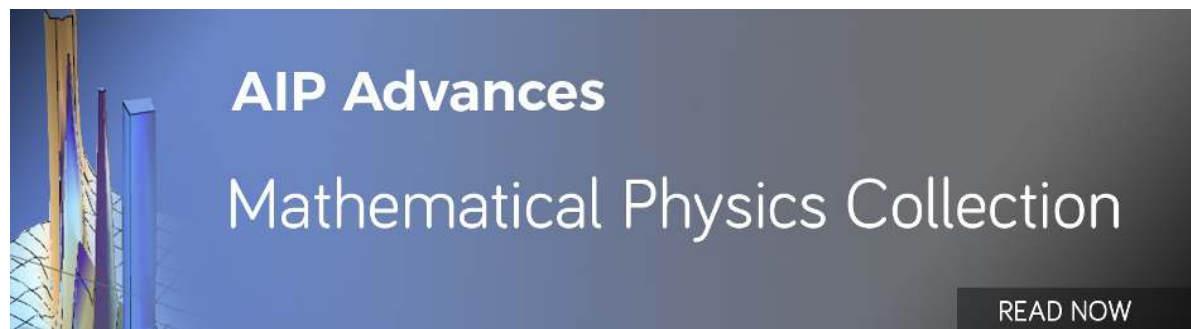
AIP Advances

Mathematical Physics Collection

READ NOW

Absence of anomalous Nernst effect in spin Seebeck effect of Pt/YIG

B. F. Miao,[1,2,a] S. Y. Huang,[2,3] D. Qu,[2] and C. L. Chien[2,b]
[1]*National Laboratory of Solid State Microstructures and Department of Physics,*
Nanjing University, Nanjing 210093, China
[2]*Department of Physics and Astronomy, Johns Hopkins University,*
Baltimore, MD 21218, USA
[3]*Department of Physics, National Taiwan University, Taipei 10617, Taiwan*

The Pt/YIG structure has been widely used to study spin Seebeck effect (SSE), inverse spin Hall effect, and other pure spin current phenomena. However, the magnetic proximity effect in Pt when in contact with YIG, and the potential anomalous Nernst effect (ANE) may compromise the spin current phenomena in Pt/YIG. By inserting a Cu layer of various thicknesses between Pt and YIG, we have separated the signals from the SSE and that of the ANE. It is demonstrated that the thermal voltage in Pt/YIG mainly comes from spin current due to the longitudinal SSE with negligible contribution from the ANE. *© 2016 Author(s). All article content, except where otherwise noted, is licensed under a Creative Commons Attribution (CC BY) license (http://creativecommons.org/licenses/by/4.0/).* [http://dx.doi.org/10.1063/1.4941340]

The ferrimagnetic insulator yttrium iron garnet (YIG = $Y_3Fe_5O_{12}$) has the unique attributes of ultra-low damping, long spin diffusion length, and the ability to accommodate pure spin currents without charge carriers.[1–3] The nonmagnetic metal Pt has also been widely used as a spin current generator and detector because of its strong spin-orbit coupling, commanding one of the largest spin Hall angles.[4–9] Together, Pt/YIG has been extensively explored in many pure spin current phenomena, including spin Hall effect, inverse spin Hall effect (ISHE), spin pumping, and longitudinal spin Seebeck effect (SSE).[2,3,10–13] Under an out-of-plane (perpendicular) temperature gradient, the longitudinal SSE in Pt/YIG enables a pure spin current injected from YIG into Pt and detected as a transverse thermal voltage through the ISHE of $\boldsymbol{E}_{ISHE} \propto \boldsymbol{J}_S \times \boldsymbol{\sigma}$, where $\boldsymbol{J}_S$ is the spin current parallel to the temperature gradient $\nabla_z T$, and $\boldsymbol{\sigma}$ is the spin index along the direction of the magnetization $\boldsymbol{M}$ of YIG.[3,14]

The magnetic proximity effect (MPE) in Pt, when Pt comes in contact with a ferromagnetic metal, such as Fe and Co, has been firmly established in the last two decades.[15–17] More recently, ample evidences including magnetoresistance (MR), anomalous Hall effect (AHE), theoretical calculation, spin pumping, and x-ray magnetic circular dichroism (XMCD) measurements, indicate that Pt also acquires induced moments when in the proximity of a ferromagnetic insulator, such as YIG.[10,12,18–20] If the polarized moments in Pt/YIG acquire anomalous Nernst effect (ANE), the pure spin current effect of SSE would be contaminated. Under a perpendicular temperature gradient $\nabla_z T$, the ANE of $\boldsymbol{E}_{ANE} \propto \nabla_Z T \times \boldsymbol{M}$ gives rise to a transverse voltage, where $\boldsymbol{M}$ is magnetization of the ferromagnet.[10,21] Both longitudinal SSE and ANE have the same field dependence and thus inseparable. Therefore, the unequivocal establishment of the longitudinal SSE in Pt/YIG is contingent upon separating the ANE contribution, if any. In this work, we address this critical question by inserting a Cu layer of various thicknesses between Pt and YIG to separate the potential contributions due to the induced moment and from that of the spin current. We show that the induced moments in Pt have negligible thermal contributions from the conventional ANE and thus the measured signal comes mainly from the longitudinal SSE.

---

[a]Electronic mail: bfmiao@nju.edu.cn
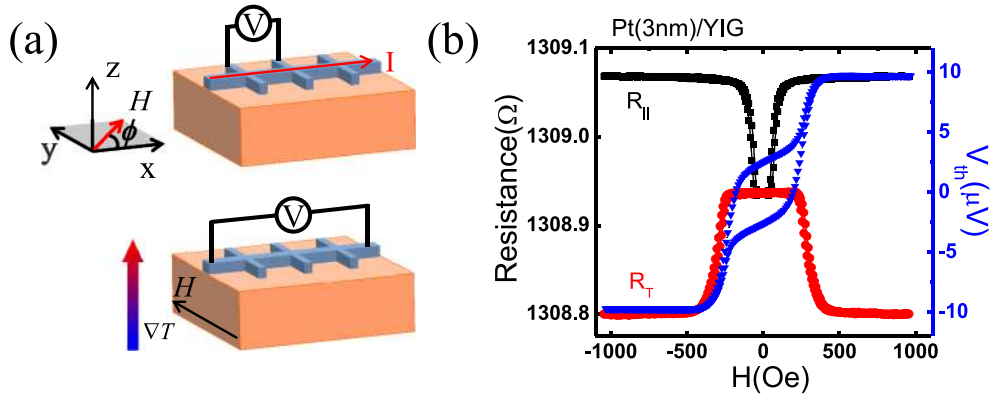[b]Electronic mail: clchien@jhu.edu

FIG. 1. (a) Schematic for the measurement of in-plane magnetoresistance. And the magnetic field is applied at an angle ϕ with respect to x-axis within xy plane. For the thermal measurent, an out-of-plane temperature gradient is applid together with a transvere field (along y-axis). (b) Field dependent longitudinal MR $R_{||}$ (black curve), transverse MR R_T (red curve), and thermal voltage V_{th} (blue curve) for Pt(3 nm)/YIG.

We use *dc* magnetron sputtering to deposit various metallic layers onto polycrystalline rectangle-shaped YIG substrates (typically 6 mm × 3 mm × 0.5 mm) at room temperature. A Cu layer of various thicknesses was placed into or onto the Pt/YIG and Au/YIG structures in the forms of Pt/Cu(t_{Cu})/YIG, Cu(t_{Cu})/Pt/YIG, and Au/Cu(t_{Cu})/YIG. We use the small angle diffraction to evaluate the film thickness and control the deposition speed. The deposited thin films have been patterned into Hall bars of width 0.2 mm with one long segment (5 mm) and three short side bars 1.5 mm apart [Fig 1(a)]. The 4-terminal method has been used to measure the MR with the magnetic field **H** applied within the xy plane at an angle ϕ with respect to the x-axis, where xyz axes are parallel to the edges of the YIG substrate with the x-axis along the long segment of the Hall bar as shown in Fig. 1(a). By placing the sample in between and in contact with two large Cu plates maintained at different constant temperatures, we apply a perpendicular temperature gradient of $\nabla_z T \approx 20$ K/mm over the whole sample. Since the YIG substrate is more than 5 orders of magnitude thicker than those of the thin films, the temperature difference is essentially established entirely within the YIG thickness. The distance between the two voltage leads for measuring the thermal voltage (V_{th}) is about 4.2 mm.

One of the distinguishing characteristics of Pt/YIG bilayer system is the appearance of the angular dependent magnetoresistance. As shown in Fig. 1(b), while Pt in isolation has no discernible MR, the Pt(3 nm)/YIG sample acquires a pronounced MR with $R_{||} > R_T$, where $R_{||}$ and R_T are the longitudinal (**M** || **I**) and the transverse (**M** ⊥ **I** and **M** oriented in the film plane) resistance, respectively. The different width of $R_{||}$ and R_T near $H = 0$ is due to the shape anisotropy of the rectangular YIG substrate; it is absent in a square YIG substrate. The MR behavior of $R_{||} > R_T$ for Pt/YIG under an in-plane field is the same as that of the well-known anisotropic magnetoresistance (AMR) in most polycrystalline ferromagnetic metals.[22] However, the key feature of the new MR is $R_\perp$ under a large out-of-plane field. The new MR shows the characteristics of $R_\perp \approx R_{||} > R_T$, altogether different from that of $R_{||} > R_T \approx R_\perp$ for AMR.[11,23,24] The difference between $R_\perp$, $R_{||}$ and R_T have a (cosine)² angular dependence due to the consequence of anisotropic conduction. This new type of MR, with unique characteristics clearly different from those of all other known MRs, has been the focus of much attention.[23–25] It was recently demonstrated that there are two physical origins of the new MR in the Pt/YIG hybrid structure, associated with the spin current across the Pt-YIG interface and the MPE at the interface.[25] The spin current contribution appears mostly in low magnetic fields, whereas the MPE contribution prevails in higher fields.[25]

In Fig. 1(b), the blue curve shows the field dependent V_{th} for Pt (3 nm)/YIG under a temperature gradient ($\nabla_z T \approx 20$ K/mm), where H is applied in the transverse direction ($\phi = 90°$). Both the V_{th} and R_T, having the same saturation field along the transverse direction, are thus clearly correlated. As mentioned earlier, the thermal voltage (V_{th}) signal with a magnitude of about 20μV may contain both SSE+ISHE ($\boldsymbol{E}_{ISHE} \propto \boldsymbol{J}_S \times \boldsymbol{\sigma}$) and ANE ($\boldsymbol{E}_{ANE} \propto \nabla_Z T \times \boldsymbol{M}$).
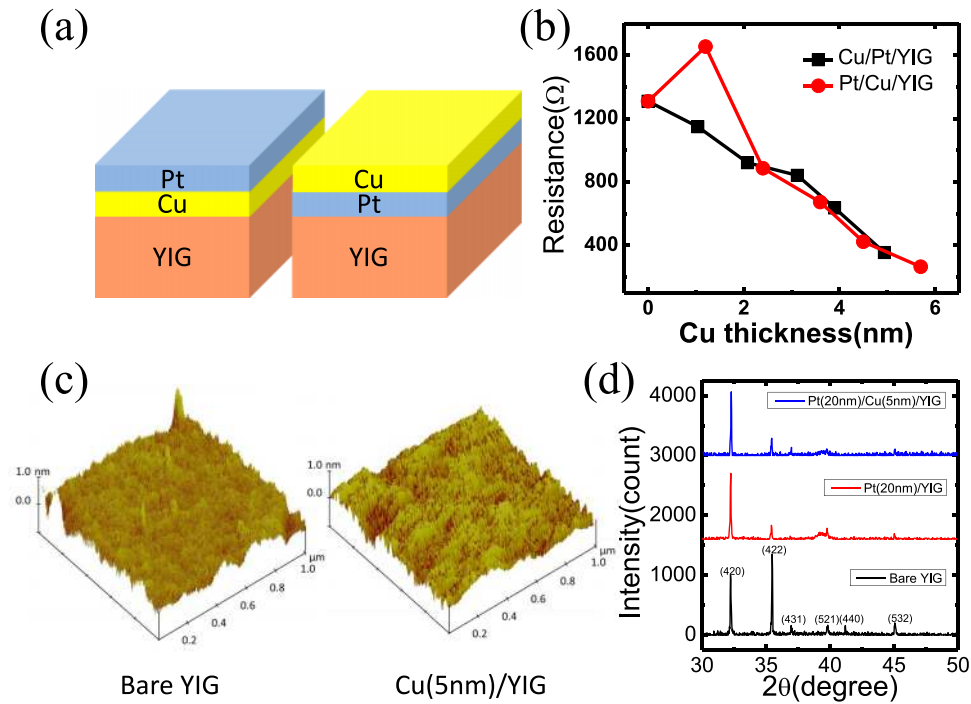
FIG. 2. (a) Schematic for the two series of samples with different thicknesses Cu as insert layer and capping layer. (b) Cu thickness dependent resistance for Pt (3 nm)/Cu (t_{Cu})/YIG (red curve) and Cu (t_{Cu})/Pt (3 nm)/ YIG (black curve) respectively. (c) Three-dimensional atomic force microscopy images of YIG substrate and YIG with 5-nm Cu film (Cu(5 nm)/YIG) respectively. (d) θ–2θ XRD scan of a YIG substrate (lower black curve), Pt(20 nm)/YIG (middle red curve) and Pt(20 nm)/Cu(5 nm)/YIG (upper blue curve), The XRD patterns have been shifted for clarify.

In order to separate the contributions of ISHE and ANE to the thermal voltage, we used a series of Pt(3 nm)/Cu(t_{Cu})/YIG samples with a Cu layer of various thicknesses inserted between Pt and YIG [Fig. 2(a)]. As the induced moment in Pt decreases with increasing Cu layer thickness, the ANE from the induced moments are expected to decay as well. However, because of the lower resistivity of the inserted Cu layers, the shunting effect would affect the electrical measurements. We therefore also measure the control samples of Cu(t_{Cu})/Pt(3 nm)/YIG [Fig. 2(a)] with the Cu layer placed on top of Pt/YIG. Figure 2(c) presents the three-dimensional atomic force microscopy images of YIG substrate and YIG with 5-nm Cu film (Cu(5nm)/YIG), which give the surface roughness for YIG and Cu(5nm)/YIG as 0. 3nm and 0.2 nm respectively. We also investigate the influence of Cu insertion layer on the structure of deposited Pt layer by X-ray diffraction (XRD). A typical θ–2θ scan of a YIG substrate is shown in Fig. 2(d) (lower black curve), with representative peaks from polycrystalline YIG. And we find the deposited 20-nm Pt film is (111)-textured polycrystalline with a broad peak locating at around 39.3 degree (middle red curve). Similar XRD pattern is also observed for Pt(20 nm)/Cu(5 nm)/YIG (upper blue curve). And there is no signature of the existence of Pt(100) in both samples. Therefore, the insertion of Cu layer does not influence the interface roughness and structure of deposited Pt films distinctly. As shown in Fig. 2(b), the resistance of the two series of samples of Pt/Cu(t_{Cu})/YIG and Cu(t_{Cu})/Pt/YIG follow the same dependence of the Cu layer thickness, excluding the lone data point for Pt/Cu(1 nm)/YIG, for which the 1 nm Cu is too thin to form a continuous film. This also indicates that the Pt films on these substrates have similar structure and grain size.

In the electrical and thermal measurements, our results show both the MR ratio and V_{th} decay with Cu thickness for the Pt/Cu/YIG and Cu/Pt/YIG samples [Fig. 3(a) and 3(b)]. However, it is important to note that the decay rates of MR ratio and V_{th} for the Pt/Cu(t_{Cu})/YIG are much larger than those for the Cu(t_{Cu})/Pt/YIG samples. The intervening Cu layer indeed plays a significant role. Since Cu/YIG has no measurable MR and Cu itself has weak spin-orbit coupling,[26,27] the $\Delta R/R$ and the thermal signals in Pt/Cu/YIG is generated within the Pt layer only. Considering a simple
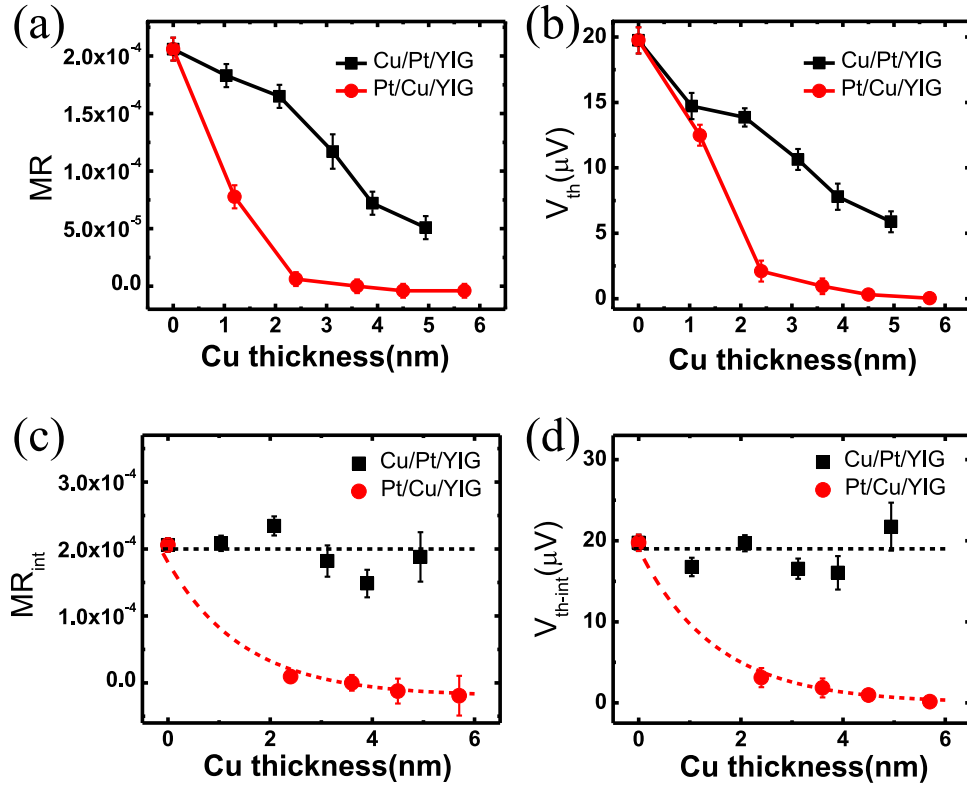
FIG. 3. Cu thickness dependent (a) MR ratio, and (b) thermal voltage V_{th} for Pt (3 nm)/Cu (t_{Cu})/YIG (red curve) and Cu (t_{Cu})/Pt (3 nm)/ YIG (black curve) respectively. (c) and (d) presents the calculated Cu thickness dependent intrinsic MR ratio and thermal voltage in Pt layer for Pt (3 nm)/Cu (t_{Cu})/YIG (red curve) and Cu (t_{Cu})/Pt (3 nm)/ YIG (black curve) respectively. The dashed lines are guides to eyes.

parallel resistor model, the resistance for the metal bilayer film of Pt(3 nm)/Cu(t_{Cu}) is approximately $R_{Pt}R(t_{Cu})/[R_{Pt} + R(t_{Cu})]$. The intrinsic MR and intrinsic thermal voltage within the Pt layer can be described as $MR_{int}(t_{Cu}) = [1 + R_{Pt}/R(t_{Cu})]MR(t_{Cu})$, $V_{th-int}(t_{Cu}) = [1 + R_{Pt}/R(t_{Cu})]V_{th}(t_{Cu})$ respectively.[23,28] For Cu (t_{Cu})/Pt(3 nm)/YIG, the intrinsic MR_{int} and V_{th-int} are nearly independent of the capping Cu layer thickness, which validates the parallel resistor model [Fig. 3(c) and 3(d)]. However, the situation is different when one reverses the layer sequence of Pt and Cu. Both the intrinsic MR_{int} and V_{th-int} have a significant thickness dependence, which decay exponentially with Cu thickness for Pt/Cu(t_{Cu})/YIG [Fig. 3(c) and 3(d)]. We note that the data point for Pt/Cu (1 nm)/YIG has been excluded in the calculation. Two possible mechanisms may account for the observed results. The spin current can decay after penetrating through the Cu insertion layer, and that the ANE due to the induced moment may diminish with the insertion of the Cu layer. We therefore resort to further experiments to distinguish these possibilities.

Unlike Pt, Au has already been demonstrated as an intrinsic spin current detector free of MPE, with no measurable MR or AHE.[18] Thus, if one performs similar experiments on a series of Au/Cu(t_{Cu})/YIG samples with different Cu thickness, one can identify the origin of the decrease of thermal voltage V_{th-int} for Pt/Cu (t_{Cu})/YIG, *i.e.,* distinguishing between the loss of spin current or induced moment in Pt. Similar to that of Pt, the V_{th-int} in Au for Au(8 nm)/Cu (t_{Cu})/YIG decays strongly with increasing the Cu insertion layer thickness [Fig. 4(a)]. Since Au has no MPE when in contact with YIG, hence no ANE, the decrease of thermal voltage in Au should solely come from the loss of spin current after penetrating through the Cu layer. We can further define a parameter of $\alpha = V_{th-int}[Cu(t\ nm)]/V_{th}[Cu(0\ nm)]$ to describe the decay rate of the thermal voltage generated within the nonmagnetic metal. Significantly, the decay rate on the Cu thickness for Au(8 nm)/Cu(t_{Cu})/YIG follows essentially the same curve as that of Pt (3 nm)/Cu(t_{Cu})/YIG in Fig. 4(b). The consistency for the two different series of samples indicates that the decrease of V_{th}
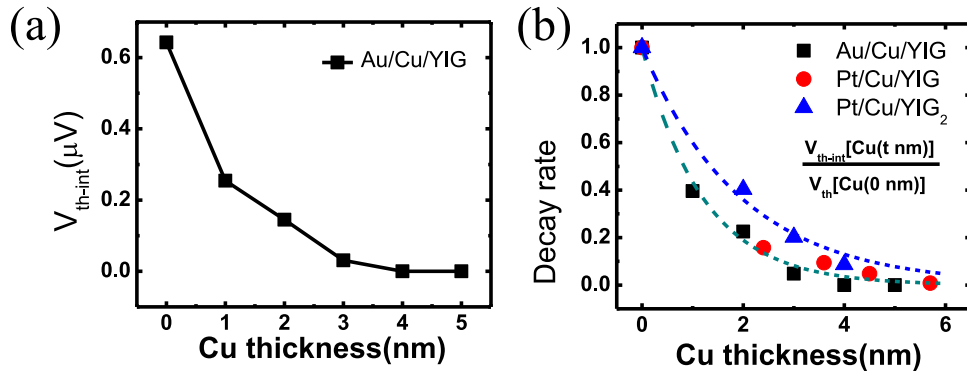
FIG. 4. (a) Cu thickness dependent intrinsic thermal signal for Au (8 nm)/Cu (t_{Cu})/YIG. (b) Cu thickness dependent decay rate V_{th-int}[Cu(t nm)]/V_{th}[Cu(0 nm)] for Au (8 nm)/Cu (t_{Cu})/YIG (black squares), Pt (3 nm)/Cu (t_{Cu})/YIG (red circles), and Pt (3 nm)/Cu (t_{Cu}/YIG$_2$ (blue triangle), where the substrate YIG$_2$ is single crystalline. The dashed line is a guide to eye.

with increasing Cu thickness is due to the loss of spin current. Therefore, the ANE from polarized Pt is negligibly small. Similar conclusion has also been made by Kikkawa *et. al.* by comparing thermal voltages in two configurations: in once case the YIG is in-plane magnetized with perpendicular temperature gradient, while in the other case the YIG is perpendicularly magnetized with in-plane temperature gradient.[29]

As indicated in Fig. 3 and Fig. 4, the characteristic length for the inserted Cu layer between Pt and YIG has been found to be 1.3 ± 0.1 nm from the exponential fit to the data. It is much shorter than the hundreds of nm observed in Cu in spin transport using lateral spin valves.[26] The short characteristic length of Cu on YIG for perpendicular spin transport leads to a rather low spin current transmission efficiency across the interface. This behavior is unlikely to be related to the polycrystalline YIG, since substantial reduction in MR ratio and V_{th} was also observed when Cu layer was inserted between Pt and single-crystalline YIG previously[23,30] and here with decay length around 2.0 nm [Fig. 4(b)]. Rather, the small characteristic length of ultra-thin Cu inserting layer is inherent to perpendicular transport, where the strong surface scattering and high resistivity are the main limiting factors. In addition, within the thickness range of interest, the spin-mixing conductances for Pt/YIG and Pt/Cu/YIG are quite similar, at least within a factor of 2, proving the similarity of interface properties.[20] So the larger than 2 orders' decrease of thermal voltage for Pt/Cu/YIG can be attributed to the loss of spin current penetrating ultra-thin Cu layer. Taking into account of the Cu thickness dependent spin-mixing conductance, the decay length for Cu in Pt/Cu/YIG slightly increases to around 1.7 nm. The short characteristic length of ultra-thin Cu has also been reported in spin pumping experiment of Pt/Cu/YIG and W/Cu/YIG,[31] as well as magnetic tunnel junctions with an interfacial Cu layer.[32,33]

In summary, we use Cu insertion layer to separate the signals from the SSE and the induced Pt moments in Pt/YIG. Through the comparative experiments between Pt/Cu(t_{Cu})/YIG and Au/Cu(t_{Cu})/YIG, we show that the thermal signal in Pt/YIG comes mainly from the longitudinal SSE with negligible contribution from the ANE, unequivocally establishing the longitudinal SSE in Pt/YIG. Finally, unlike that in lateral spin transport, the spin signal decays strongly in perpendicular spin transport across the thin Cu layer as observed in both polycrystalline and single crystal YIG substrates.

[1] M. Sparks, *Ferromagnetic-Relaxation Theory* (McGraw Hill, New York, 1964).
[2] Y. Kajiwara, K. Harii, S. Takahashi, J. Ohe, K. Uchida, M. Mizuguchi, H. Umezawa, H. Kawai, K. Ando, K. Takanashi, S. Maekawa, and E. Saitoh, Nature **464**, 262 (2010).

[3] K.-i. Uchida, H. Adachi, T. Ota, H. Nakayama, S. Maekawa, and E. Saitoh, Appl. Phys. Lett. **97**, 172505 (2010).

[4] T. Kimura, Y. Otani, T. Sato, S. Takahashi, and S. Maekawa, Phys. Rev. Lett. **98**, 156601 (2007).

[5] O. Mosendz, J. E. Pearson, F. Y. Fradin, G. E. Bauer, S. D. Bader, and A. Hoffmann, Phys. Rev. Lett. **104**, 046601 (2010).

[6] O. Mosendz, V. Vlaminck, J. E. Pearson, F. Y. Fradin, G. E. W. Bauer, S. D. Bader, and A. Hoffmann, Phys. Rev. B **82**, 214403 (2010).

[7] A. Azevedo, L. H. Vilela-Leão, R. L. Rodríguez-Suárez, A. F. Lacerda Santos, and S. M. Rezende, Phys. Rev. B **83**, 144402 (2011).

[8] Z. Feng, J. Hu, L. Sun, B. You, D. Wu, J. Du, W. Zhang, A. Hu, Y. Yang, D. M. Tang, B. S. Zhang, and H. F. Ding, Phys. Rev. B **85**, 214423 (2012).

[9] L. Liu, T. Moriyama, D. C. Ralph, and R. A. Buhrman, Phys. Rev. Lett. **106**, 036601 (2011).

[10] S. Y. Huang, X. Fan, D. Qu, Y. P. Chen, W. G. Wang, J. Wu, T. Y. Chen, J. Q. Xiao, and C. L. Chien, Phys. Rev. Lett. **109**, 107204 (2012).

[11] C. Hahn, G. de Loubens, O. Klein, M. Viret, V. V. Naletov, and J. Ben Youssef, Phys. Rev. B **87**, 174417 (2013).

[12] M. Weiler, M. Althammer, F. D. Czeschka, H. Huebl, M. S. Wagner, M. Opel, I.-M. Imort, G. Reiss, A. Thomas, R. Gross, and S. T. B. Goennenwein, Phys. Rev. Lett. **108**, 106602 (2012).

[13] O. Allivy Kelly, A. Anane, R. Bernard, J. Ben Youssef, C. Hahn, A. H. Molpeceres, C. Carrétéro, E. Jacquet, C. Deranlot, P. Bortolotti, R. Lebourgeois, J.-C. Mage, G. de Loubens, O. Klein, V. Cros, and A. Fert, Appl. Phys. Lett. **103**, 082408 (2013).

[14] B. F. Miao, S. Y. Huang, D. Qu, and C. L. Chien, Phys. Rev. Lett. **111**, 066602 (2013).

[15] F. Wilhelm, P. Poulopoulos, A. Scherz, H. Wende, K. Baberschke, M. Angelakeris, N. K. Flevaris, J. Goulon, and A. Rogalev, Phys. Status Solidi A **196**, 33 (2003).

[16] F. Wilhelm, P. Poulopoulos, G. Ceballos, H. Wende, K. Baberschke, P. Srivastava, D. Benea, H. Ebert, M. Angelakeris, N. K. Flevaris, D. Niarchos, A. Rogalev, and N. B. Brookes, Phys. Rev. Lett. **85**, 413 (2000).

[17] J. Geissler, E. Goering, M. Justen, F. Weigand, G. Schütz, J. Langer, D. Schmitz, H. Maletta, and R. Mattheis, Phys. Rev. B **65**, 020405 (2001).

[18] D. Qu, S. Y. Huang, J. Hu, R. Wu, and C. L. Chien, Phys. Rev. Lett. **110**, 067206 (2013).

[19] Y. M. Lu, Y. Choi, C. M. Ortega, X. M. Cheng, J. W. Cai, S. Y. Huang, L. Sun, and C. L. Chien, Phys. Rev. Lett. **110**, 147207 (2013).

[20] Y. Sun, H. Chang, M. Kabatek, Y.-Y. Song, Z. Wang, M. Jantz, W. Schneider, M. Wu, E. Montoya, B. Kardasz, B. Heinrich, S. G. E. te Velthuis, H. Schultheiss, and A. Hoffmann, Phys. Rev. Lett. **111**, 106601 (2013).

[21] W. Nernst, Annalen der Physik **267**, 760 (1887).

[22] T. R. McGuire and R. I. Potter, IEEE Trans. Magn. **11**, 1018 (1975).

[23] H. Nakayama, M. Althammer, Y. T. Chen, K. Uchida, Y. Kajiwara, D. Kikuchi, T. Ohtani, S. Geprägs, M. Opel, S. Takahashi, R. Gross, G. E. W. Bauer, S. T. B. Goennenwein, and E. Saitoh, Phys. Rev. Lett. **110**, 206601 (2013).

[24] Y. M. Lu, J. W. Cai, S. Y. Huang, D. Qu, B. F. Miao, and C. L. Chien, Phys. Rev. B **87**, 220409 (2013).

[25] B. F. Miao, S. Y. Huang, D. Qu, and C. L. Chien, Phys. Rev. Lett. **112**, 236601 (2014).

[26] T. Kimura, J. Hamrle, and Y. Otani, Phys. Rev. B **72**, 014461 (2005).

[27] H. L. Wang, C. H. Du, Y. Pu, R. Adur, P. C. Hammel, and F. Y. Yang, Phys. Rev. Lett. **112**, 197201 (2014).

[28] H. Nakayama, K. Ando, K. Harii, T. Yoshino, R. Takahashi, Y. Kajiwara, K. Uchida, Y. Fujikawa, and E. Saitoh, Phys. Rev. B **85**, 144408 (2012).

[29] T. Kikkawa, K. Uchida, S. Daimon, Y. Shiomi, H. Adachi, Z. Qiu, D. Hou, X. F. Jin, S. Maekawa, and E. Saitoh, Phys. Rev. B **88**, 214403 (2013).

[30] T. Kikkawa, K. Uchida, Y. Shiomi, Z. Qiu, D. Hou, D. Tian, H. Nakayama, X. F. Jin, and E. Saitoh, Phys. Rev. Lett. **110**, 067207 (2013).

[31] C. Du, H. Wang, F. Yang, and P. C. Hammel, Phys. Rev. Applied **1**, 044004 (2014).

[32] P. LeClair, H. J. M. Swagten, J. T. Kohlhepp, R. J. M. van de Veerdonk, and W. J. M. de Jonge, Phys. Rev. Lett. **84**, 2933 (2000).

[33] P. LeClair, J. T. Kohlhepp, H. J. M. Swagten, and W. J. M. de Jonge, Phys. Rev. Lett. **86**, 1066 (2001).